1^{st} year PhD report

Mauro D'Arcangelo
Supervisor: Prof. J. W. Barrett

Contents

1 Introduction

This project is concerned with the characterization of *random fuzzy spaces* by means of Markov chain Monte Carlo simulations. The chapter presents a brief introduction to the basic concepts (non-commutative, fuzzy and random).

1.1 Non-commutative geometry

The fundamental object of non-commutative geometry is a *spectral triple* (A, H, D) where A is an algebra with a representation in a Hilbert space H and D is an operator on H, called Dirac operator. A Riemannian spin manifold can be fully characterized by the commutative algebra A of functions on the manifold and by the Dirac operator, which encodes the metric [11] [10]. One could then consider a generalization in which the algebra is allowed to be non-commutative. Such geometries arise naturally in physics, and are tightly related to gauge theories [20]. Indeed it has been shown that the Standard Model has the structure of a non-commutative geometry [7] [1] [8]. This suggests a possible path to quantum gravity by replacing the ordinary commutative spacetime by a non-commutative one that presents a commutative behaviour as a limiting case.

1.2 Fuzzy spaces

There is a class of non-commutative geometries called *fuzzy spaces*, where the algebra is taken to be $M_n(\mathbb{C})$, the algebra of $n \times n$ complex matrices, and the Hilbert space is finite dimensional. The Dirac operator of a fuzzy space takes the form [2]:

$$D = \sum_j \alpha_j \otimes [L_j, \cdot] + \sum_k \tau_k \otimes \{H_k, \cdot\} \tag{1}$$

where:

1. τ_k and α_j are respectively Hermitian and anti-Hermitian basis elements of the algebra generated by a (p, q) Clifford module;

2. H_k and L_j are $n \times n$ Hermitian and anti-Hermitian matrices respectively;

3. $[\cdot,\cdot]$ indicates a commutator and $\{\cdot,\cdot\}$ an anti-commutator.

Fuzzy spaces are classified by the pair of integers (p, q) of the Clifford module. It is worth noting that any choice of H_k and L_j gives an admissible Dirac operator, as long as the Hermitian or anti-Hermitian character is preserved. See Appendix A for some remarks on the notation used.

1.3 Random geometries

A *random geometry* is a spectral triple (A, H, D) in which the Dirac operator fluctuates according to a certain probability measure. Here the probability measure is taken to be proportional to:

$$e^{-S[D]}dD \tag{2}$$

for a certain choice of $S[D]$. The expectation value of an observable $f(D)$ on a random geometry is given by:

$$\langle f(D)\rangle = \int f(D)e^{-S[D]}dD. \tag{3}$$

Since D encodes the metric, this is in clear analogy with the Euclidean path integral of Quantum Field Theory.
So far no assumption has been made on the choice of Dirac operator. The purpose of this project is to study the path integral when D is taken to be the Dirac operator of a fuzzy space.
Fuzzy spaces provide an alternative type of regularization that is non-lattice [3]. Therefore the study of such random geometries is especially interesting in connection with models of (Euclidean) quantum gravity.
This line of research first appeared in [3], where the following action was considered:

$$S[D] = g_2 \operatorname{Tr} D^2 + \operatorname{Tr} D^4, \quad g_2 \in \mathbb{R}. \tag{4}$$

In the remainder, the action is taken to be of the form of Eq.(4).
The expectation value (3) is computed numerically using Monte Carlo methods. Eq.(3) is therefore replaced by:

$$\langle f(D)\rangle \approx \frac{1}{N}\sum_{i=1}^{N} f(D_i) \tag{5}$$

where $\{D_i\}$ is a set of Dirac operators sampled from the distribution (2).

2 Results

2.1 Improvements in the numerical algorithm

The evaluation of integrals such as (3) requires a way to sample the most relevant configurations (the *typical set*) out of the entirety of parameter space. The simplest algorithm based on Markov chains for doing so is Metropolis-Hastings [17]. Two crucial shortcomings of Metropolis are a rather slow exploration of the typical set based on a random walk in parameter space, and the large correlation between adjacent samples. A more sophisticated approach is Hybrid Monte Carlo, or HMC XXXX(duane): originally developed for lattice QCD computations, it allows a faster and more uniform exploration of the typical set by transposing the problem of sampling from a distribution to Hamiltonian evolution in a fictitious phase space.
After a brief explanation of the idea behind HMC, the adaptation to the fuzzy space path integral is discussed and the results from numerical simulations are presented with a comparison between HMC and Metropolis.

2.1.1 Hybrid Monte Carlo

In Markov chain theory one is interested in a system specified by a finite set of parameters $(q_1, \cdots, q_N)$, $q_i \in \mathbb{R}$, collectively referred to as $\mathbf{q}$. The probability that the system be in a particular configuration is given by some probability measure $\pi(\mathbf{q})d\mathbf{q}$. Given an initial configuration $\mathbf{q}$, a Markov chain establishes a transition $\mathbf{q} \to \mathbf{q}'$ from the old configuration to a new one in such a way that $\mathbf{q}'$ is chosen with the desired probability.
This situation is analogous to the Monte Carlo estimation of the integral (3), where the parameters are the independent degrees of freedom of the Dirac operator and the probability measure is $e^{-S[D]}dD$.
The first step of Hybrid Monte Carlo is to enlarge parameter space by introducing a "conjugate momentum" p_i to each parameter q_i, thus effectively working in a fictitious phase space. The probability measure is extended to include the new variables $\pi(\mathbf{q}) \to \pi(\mathbf{q}, \mathbf{p})$. By defining the "Hamiltonian" $H(\mathbf{q}, \mathbf{p}) \equiv -\log \pi(\mathbf{q}, \mathbf{p})$, a configuration is then evolved along a Hamiltonian trajectory by integrating Hamilton's equations:

$$\frac{dq_i}{dt} = \frac{\partial H}{\partial p_i} \tag{6}$$

$$\frac{dp_i}{dt} = -\frac{\partial H}{\partial q_i} \tag{7}$$

where t denotes a fictitious time that will be referred to as Monte Carlo time. This specifies a transition $(\mathbf{q}(0), \mathbf{p}(0)) \to (\mathbf{q}(t), \mathbf{p}(t))$ from an initial

configuration to a new one. The new configuration is then accepted with probability $\min[1, \exp(H(t) - H(0))]$.
Note that Hamiltonian dynamics preserves the value of the energy of the system, therefore $H(t) = H(0)$ and $\min[1, \exp(H(t) - H(0))] = 1$. However, numerical integration of Hamilton's equations is a non-trivial matter that introduces errors, therefore $H(t) \neq H(0)$ in general. The standard choice of numerical integrator in HMC is the so-called *leapfrog* integrator. For details see Appendix ZZZZ.

2.1.2 Adapting HMC to fuzzy spaces

In the matrix integral considered here, the dynamical variables are the $n \times n$ Hermitian matrices M_i, to which a corresponding set of Hermitian matrices P_i is added. The Hamiltonian is chosen to be simply:

$$H(M_i, P_i) = S[M_i] + \sum_i \frac{1}{2} P_i^2. \tag{8}$$

Schematically, the algorithm goes as follows:

1. extract the momenta P_i according to $\exp(-P_i^2/2)$;
2. integrate Hamilton's equations for a certain time t;
3. accept the new configuration with probability $\min[1, \exp(H(t) - H(0))]$.

The non-trivial step in the leapfrog integrator is the evaluation of the force term in Eq.(YYYY), which requires to take derivatives such as:

$$\frac{\partial S[M_i]}{\partial M_k} \tag{9}$$

which amounts to finding formulas for terms like:

$$\frac{\partial \operatorname{Tr} D(M_i)^p}{\partial M_k}. \tag{10}$$

For the definition of matrix derivative see Appendix B. In the following, formulas for $p = 2$ and $p = 4$ are developed.

2.1.3 The case $p = 2$

When $p = 2$ the M_i matrices are decoupled:

$$\operatorname{Tr} D^2 = \sum_i \operatorname{Tr} \omega_i^2 (2n \operatorname{Tr} M_i^2 + 2\epsilon_i (\operatorname{Tr} M_i)^2). \tag{11}$$

Taking a derivative with respect to M_k yields:

$$\frac{\partial}{\partial M_k}\left(\sum_i \operatorname{Tr}\omega_i^2(2n\operatorname{Tr}M_i^2+2\epsilon_i(\operatorname{Tr}M_i)^2)\right) =$$
$$\sum_i \delta_{ik}\operatorname{Tr}\omega_i^2\left(4nM_i^T+4\epsilon_i(\operatorname{Tr}M_i)I\right) =$$
$$4C\left(nM_k^T+\epsilon_k(\operatorname{Tr}M_k)I\right) \tag{12}$$

where $C \equiv \operatorname{Tr}\omega_i^2$ is the dimension of the Clifford module.

2.1.4 The case $p = 4$

First expand $\operatorname{Tr}D^4$:

$$\begin{aligned}\operatorname{Tr}D^4 = \sum_{i_1,i_2,i_3,i_4} &\operatorname{Tr}(\omega_{i_1}\omega_{i_2}\omega_{i_3}\omega_{i_4})\cdot \\ \Big(& n[1+\epsilon *]\operatorname{Tr}(M_{i_1}M_{i_2}M_{i_3}M_{i_4}) \;+ \\ & \epsilon_{i_1}\operatorname{Tr}M_{i_1}[1+\epsilon *]\operatorname{Tr}(M_{i_2}M_{i_3}M_{i_4}) \;+ \\ & \epsilon_{i_2}\operatorname{Tr}M_{i_2}[1+\epsilon *]\operatorname{Tr}(M_{i_1}M_{i_3}M_{i_4}) \;+ \\ & \epsilon_{i_3}\operatorname{Tr}M_{i_3}[1+\epsilon *]\operatorname{Tr}(M_{i_1}M_{i_2}M_{i_4}) \;+ \\ & \epsilon_{i_4}\operatorname{Tr}M_{i_4}[1+\epsilon *]\operatorname{Tr}(M_{i_1}M_{i_2}M_{i_3}) \;+ \\ & \epsilon_{i_1}\epsilon_{i_2}[1+\epsilon]\operatorname{Tr}(M_{i_1}M_{i_2})\operatorname{Tr}(M_{i_3}M_{i_4}) \;+ \\ & \epsilon_{i_1}\epsilon_{i_3}[1+\epsilon]\operatorname{Tr}(M_{i_1}M_{i_3})\operatorname{Tr}(M_{i_2}M_{i_4}) \;+ \\ & \epsilon_{i_1}\epsilon_{i_4}[1+\epsilon]\operatorname{Tr}(M_{i_1}M_{i_4})\operatorname{Tr}(M_{i_2}M_{i_3}) \Big)\end{aligned} \tag{13}$$

where $*$ denotes complex conjugation of everything that appears on the right, ϵ is defined as the product $\epsilon \equiv \epsilon_{i_1}\epsilon_{i_2}\epsilon_{i_3}\epsilon_{i_4}$, and the relation $M^T = M^*$ has been used. Since D is Hermitian, the expression must be real. It is not immediate to see that this is the case because of the $\epsilon = \pm 1$ factor inside the square brackets. Reality nonetheless holds, and becomes manifest by observing that a simultaneous index exchange $i_1 \leftrightarrow i_4$ and $i_2 \leftrightarrow i_3$ is equivalent to taking the complex conjugate (in fact, this is not the only index exchange that amounts to complex conjugation).
Taking a matrix derivative with respect to M_k results in non-vanishing con-

tributions when $k = i_1, k = i_2, k = i_3$ or $k = i_4$:

$$\frac{\partial}{\partial M_k} \operatorname{Tr} D^4 = \sum_{i_1,i_2,i_3,i_4} \operatorname{Tr}(\omega_{i_1}\omega_{i_2}\omega_{i_3}\omega_{i_4}) \cdot \Big(\delta_{ki_1} A(i_1,i_2,i_3,i_4)^T + \delta_{ki_2} A(i_2,i_3,i_4,i_1)^T + \delta_{ki_3} A(i_3,i_4,i_1,i_2)^T + \delta_{ki_4} A(i_4,i_1,i_2,i_3)^T\Big) \tag{14}$$

where $A(a,b,c,d)$ is the following $n \times n$ matrix:

$$\begin{aligned} A(a,b,c,d) \equiv\ & n[1+\epsilon\ \dagger] M_b M_c M_d + \\ & \epsilon_a I [1+\epsilon\ *] \operatorname{Tr} M_b M_c M_d + \\ & \epsilon_b \operatorname{Tr} M_b [1+\epsilon\ \dagger] M_c M_d + \\ & \epsilon_c \operatorname{Tr} M_c [1+\epsilon\ \dagger] M_b M_d + \\ & \epsilon_d \operatorname{Tr} M_d [1+\epsilon\ \dagger] M_b M_c + \\ & \epsilon_a \epsilon_b M_b [1+\epsilon] \operatorname{Tr} M_c M_d + \\ & \epsilon_a \epsilon_c M_c [1+\epsilon] \operatorname{Tr} M_b M_d + \\ & \epsilon_a \epsilon_d M_d [1+\epsilon] \operatorname{Tr} M_b M_c \end{aligned} \tag{15}$$

and $\dagger$ denotes Hermitian conjugation of everything that appears on the right. Upon relabeling the indices and cycling the ω matrices in the trace, the equation becomes:

$$\begin{aligned} \frac{\partial}{\partial M_k} \operatorname{Tr} D^4 &= 4 \sum_{i_1,i_2,i_3,i_4} \delta_{ki_1} \operatorname{Tr}(\omega_{i_1}\omega_{i_2}\omega_{i_3}\omega_{i_4}) A(i_1,i_2,i_3,i_4)^T \\ &= 4 \sum_{i_1,i_2,i_3} \operatorname{Tr}(\omega_k \omega_{i_1}\omega_{i_2}\omega_{i_3}) A(k,i_1,i_2,i_3)^T \equiv 4 \sum_{i_1,i_2,i_3} \mathcal{B}_k(i_1,i_2,i_3) \end{aligned} \tag{16}$$

with $\mathcal{B}_k(a,b,c)$ denoting the generic term in the sum.
To see that Eq.(16) defines a Hermitian matrix, notice that an exchange of indices $i_1 \leftrightarrow i_3$ is equivalent to taking the Hermitian conjugate:

$$\mathcal{B}_k(i_1,i_2,i_3)^\dagger = \mathcal{B}_k(i_3,i_2,i_1) \tag{17}$$

therefore the sum in Eq.(16) reduces to:

$$\sum_{\substack{i_1 > i_3 \\ i_2}} [1+\dagger] \mathcal{B}_k(i_1,i_2,i_3) + \sum_{i_1,i_2} \mathcal{B}_k(i_1,i_2,i_1). \tag{18}$$

In fact, by looking at the form of $\mathcal{B}$, it is clear that terms in the sum are qualitatively different based on the number of indices that coincide. Therefore it would be computationally convenient to write Eq.(18) in a way that emphazises this difference.
The only terms that contribute when all indices are different are the following:

$$\sum_{i_1>i_2>i_3} [1+\dagger]\Big(\mathcal{B}_k(i_1,i_2,i_3)+\mathcal{B}_k(i_1,i_3,i_2)+\mathcal{B}_k(i_2,i_1,i_3)\Big). \tag{19}$$

The three inequivalent permutations of indices that appear in this formula are based on a group-theoretical argument that will generalize easily to powers of D higher than 4. First consider the symmetric group of order three S_3 acting on the set of indices $\{i_1,i_2,i_3\}$, and the subgroup of permutations that induce a simple change in $\mathcal{B}$, which in this case is $H=\{(),(13)\}\cong S_2$ (the first element being the identical permutation, and the second the exchange $i_1\leftrightarrow i_3$ which induces $\mathcal{B}\to\mathcal{B}^\dagger$). The idea is then to restrict the sum to $i_1>i_2>i_3$ and quotient out the action of H by introducing a suitable pre-factor that accounts for it (in this case $[1+\dagger]$). Practically, the inequivalent permutations of indices that appear in Eq.(19) are found by computing the (left or right) cosets of $H\subset S_3$ and acting on $\{i_1,i_2,i_3\}$ with a representative from each coset. In this case the representatives where chosen to be $(),(23),(12)$.
What is left are terms in which at least two indices are equal. These are:

$$\sum_{i_1>i_2}[1+\dagger]\Big(\mathcal{B}_k(i_1,i_1,i_2)+\mathcal{B}_k(i_1,i_2,i_2)\Big)+ \\ \sum_{i_1\neq i_2}\mathcal{B}_k(i_1,i_2,i_1)+\sum_i\mathcal{B}_k(i,i,i). \tag{20}$$

At this point, a useful property of the ω matrices can be exploited to simplify both Eq.(19) and Eq.(20):

$$\operatorname{Tr}(\omega_{\sigma(i_1)}\omega_{\sigma(i_2)}\omega_{\sigma(j)}\omega_{\sigma(k)})\propto\operatorname{Tr}(\omega_j\omega_k)=0 \qquad \text{if } \ i_1=i_2 \text{ and } j\neq k \tag{21}$$

for any permutation σ acting on $\{i_1,i_2,j,k\}$. In other words, if two indices are the same and the other two are different, the trace on the ω matrices vanishes.
Putting together Eq.(19), Eq.(20) and Eq.(21), the final formula for $\partial_k\operatorname{Tr}D^4$

reads:

$$\frac{\partial}{\partial M_k} \operatorname{Tr} D^4 = 4\Bigg[\sum_{\substack{i_1>i_2>i_3 \\ i_1,i_2,i_3\neq k}} [1+\dagger]\Big(\mathcal{B}_k(i_1,i_2,i_3)+\mathcal{B}_k(i_1,i_3,i_2)+\mathcal{B}_k(i_2,i_1,i_3)\Big) \\ + \sum_{\substack{i \\ i\neq k}} \Big([1+\dagger]\mathcal{B}_k(i,i,k)+\mathcal{B}_k(i,k,i)\Big)+\mathcal{B}_k(k,k,k)\Bigg]. \tag{22}$$

The explicit form of $\mathcal{B}_k(i,i,k)$, $\mathcal{B}_k(i,k,i)$ and $\mathcal{B}_k(k,k,k)$ is given in Appendix C.

2.1.5 Testing HMC against exact results

Although not many analytical results are available for the matrix integrals considered here, there is a non-trivial observable whose expectation value is known exactly for any geometry and any action polinomial in D. Computing this observable therefore provides a good test for the numerical implementation.
Consider the following vanishing integral:

$$0 = \int \frac{\partial}{\partial D_{ij}} \left(D_{ij} e^{-S[D]}\right) dD \tag{23}$$

where D_{ij} is one of the non-zero components of the Dirac operator and $S[D]$ is in general sum of terms like $g_p \operatorname{Tr} D^p$. An explicit calculation of the partial derivative on these traces gives:

$$\frac{\partial}{\partial D_{ij}} \operatorname{Tr} D^p = \frac{\partial}{\partial D_{ij}} \sum_{a_1,\cdots,a_p} D_{a_1a_2}\cdots D_{a_pa_1} = p\ m_{ij} \sum_{a_2,\cdots,a_p} D_{ja_2}\cdots D_{a_pi} \tag{24}$$
$$= p\ m_{ij}(D^{p-1})_{ji}$$

where m_{ij} counts the multiplicity of the component D_{ij} in the Dirac operator (recall that the Dirac operator is heavily constrained and not all the non-vanishing components are independent degrees of freedom). The integral (23) then becomes:

$$0 = \int \frac{\partial}{\partial D_{ij}} \left(D_{ij} e^{-S[D]}\right) dD = \int \left(1 - \sum_p g_p\ p\ m_{ij} D_{ij} (D^{p-1})_{ji}\right) e^{-S[D]} dD \tag{25}$$

dividing by the partition function then gives:

$$1 = \frac{1}{\int e^{-S[D]}} \int \left(\sum_p g_p \; p \; m_{ij} D_{ij} (D^{p-1})_{ji} \right) e^{-S[D]} dD \tag{26}$$

and finally summing over all i, j corresponding to independent degrees of freedom:

$$\#\text{d.o.f.}(D) = \frac{1}{\int e^{-S[D]}} \int \left(\sum_p g_p \; p \operatorname{Tr} D^p \right) e^{-S[D]} dD = \left\langle \sum_p g_p \; p \; \operatorname{Tr} D^p \right\rangle \tag{27}$$

2.2 Phase transitions and order parameters

In [3] the first indication of a phase transition was found for geometries that have H matrices in the Dirac operator. An order parameter for the phase transition was also proposed:

$$F \equiv \frac{\sum_i (\operatorname{Tr} H_i)^2}{n \sum_i \operatorname{Tr} H_i^2}. \tag{28}$$

In [12] F was used in a Finite Size Scaling analysis for the $(2,0)$ geometry (see section 2.7 for developments in this area).
In order to interpret the observable F, it is useful to look at the $(2,0)$ geometry explicitly. In this case F is:

$$F_{(2,0)} = \frac{(\operatorname{Tr} H_1)^2 + (\operatorname{Tr} H_2)^2}{n(\operatorname{Tr} H_1^2 + \operatorname{Tr} H_2^2)}. \tag{29}$$

In a plot of $\operatorname{Tr} H_1$ vs $\operatorname{Tr} H_2$ before, during and after the phase transition, it is clear that the observable F can be interpreted as the square of the radius of a circle (Fig.(5)). The behaviour for F was then analized systematically for higher geometries. The results are reported in Fig.(6).
It seems to be the case that phase transitions in fuzzy spaces are driven by F developing a non-zero expectation value. However, in the next section it will be shown that in the case of the $(1,3)$ geometry an alternative observable built on the L matrices behaves like an order parameter for the phase transition. The implications of this dual description have not yet been object of study.

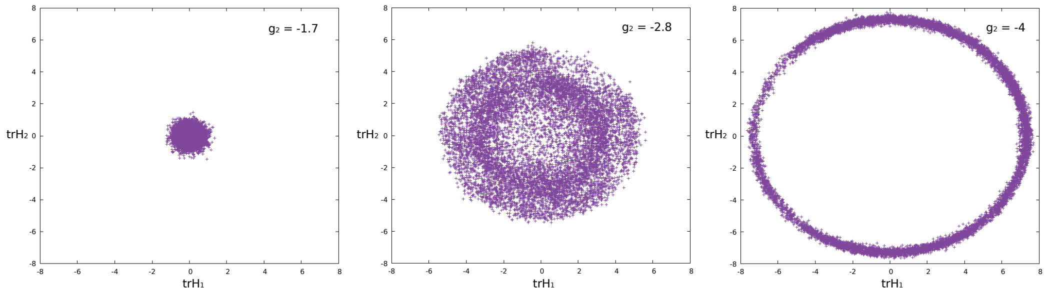

Figure 1: From left to right: $\operatorname{Tr} H_1$ vs $\operatorname{Tr} H_2$ before, during and after the $(2,0)$ phase transition. Each point denotes a Monte Carlo step.

2.3 Algebraic structures forming in the $(1,3)$ phase transition

It has been argued in [3] that random fuzzy geometries might present a manifold-like behaviour close to phase transitions in the limit of infinite matrix size. A natural candidate for investigating this possibility is the $(1,3)$ random fuzzy space: it exhibits a phase transition [16] and it contains the fuzzy sphere as a particular case [2].
The most general Dirac operator of a $(1,3)$ fuzzy space is:

$$D_{13} = \gamma^0 \otimes \{H_0, \cdot\} + \gamma^1\gamma^2\gamma^3 \otimes \{H_{123}, \cdot\} + \sum_{i=1}^{3} \gamma^i \otimes [L_i, \cdot] + \sum_{j<k=1}^{3} \gamma^0\gamma^j\gamma^k \otimes [L_{jk}, \cdot] \tag{30}$$

where γ^0, γ^1, γ^2, γ^3 are the gamma matrices of an irreducible $(1,3)$ Clifford module (γ^0 is the Hermitian one).
The Dirac operator of a fuzzy sphere is:

$$D_{fs} = \gamma^0 \otimes I + \sum_{j<k=1}^{3} \gamma^0\gamma^j\gamma^k \otimes [L_{jk}, \cdot] \tag{31}$$

where L_{jk} are the standard generators of an irreducible n-dimensional representation of the Lie algebra $so(3)$.
A priori, when considering a random Dirac operator of the form D_{13}, the smallest algebra in which the L_{jk} matrices live is much bigger than $so(3)$. But if D_{13} is to resemble D_{fs} at the phase transition, then one would expect the algebra to shrink. In particular, the angle between $[L_{jk}, L_{lm}]$ and L_{pq} should decrease.
In order to test this hypotesis, every inequivalent angle† between $[L_\alpha, L_\beta]$ and

†The angle was defined using the Frobenius inner product: $\langle A, B\rangle = \operatorname{Tr} A^\dagger B$

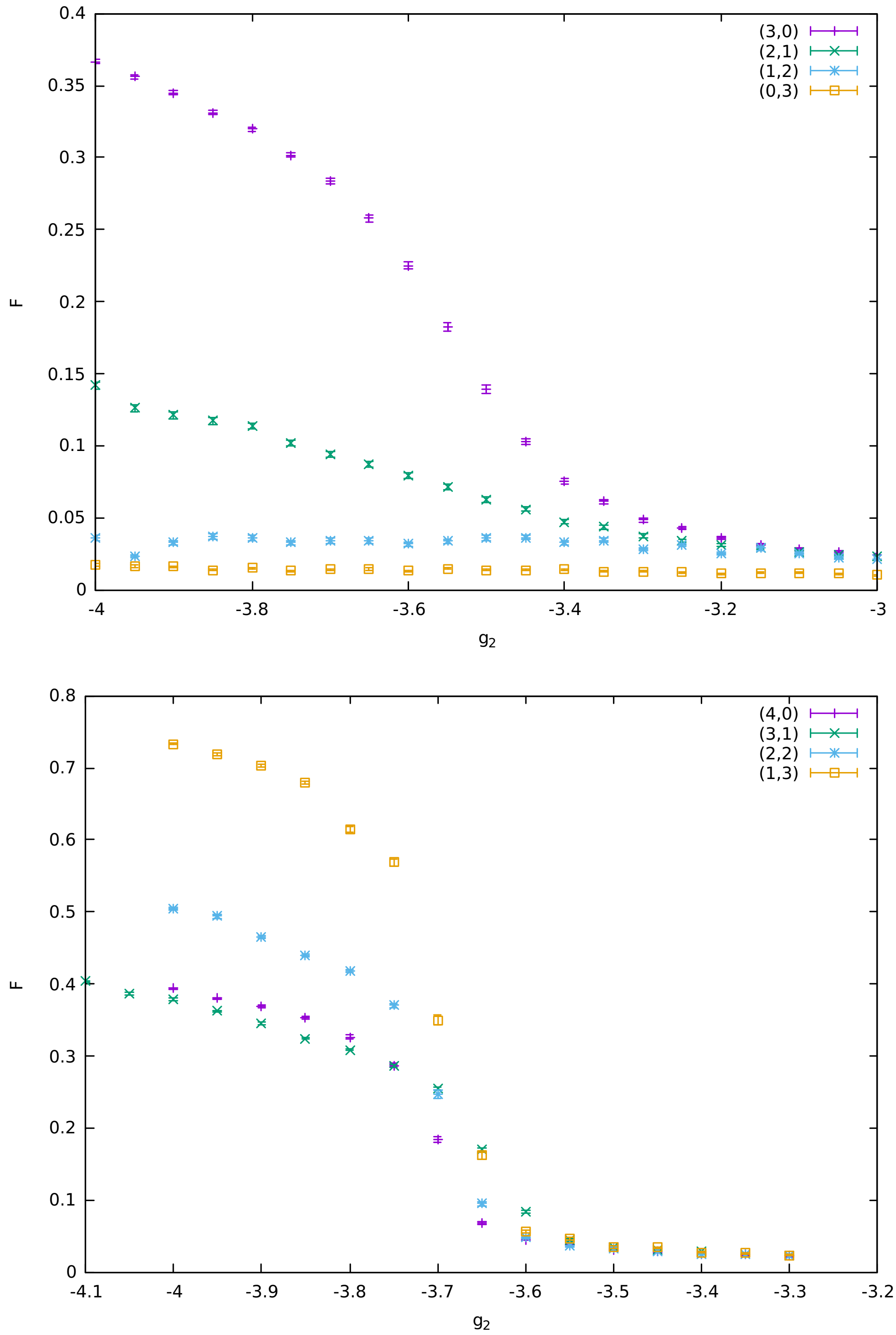

Figure 2: Observable F for $p+q = 3$ (top) and $p+q = 4$ geometries (bottom). Matrix size is 8×8.

L_γ has been measured close to the critical point, where L_α, L_β, L_γ are any of the L_i or L_{jk} matices of Eq.(34).
The results shown in Fig.(7) suggest that the three L_i matrices and the three L_{jk} matrices naturally split in two groups, and that in each group the angle at the phase transition decreases more and more as the matrix size increases.

2.4 The $(2, 0)$ double jump phase transition

The $(2, 0)$ fuzzy space is a useful toy model to explore the behaviour of random fuzzy spaces. In [12] the $(2, 0)$ phase transition was studied by means of Finite Size Scaling. The results were compatible with the phase transition being in the universality class of the 3D Ising model or the 3D XY model.
The previous study was conducted with matrices up to size 15×15. In an attempt to better constrain the values of the critical exponents, new simulations have been perfomed with matrices of size 20×20, 25×25 and 30×30.
The new data (Fig.(8)) shows that the phase transition has in fact a richer structure, with a double jump. This feature is not observed in 3D Ising or XY model.

2.5 Phase transitions and order parameters

In [3] the first indication of a phase transition was found for geometries that have H matrices in the Dirac operator. An order parameter for the phase transition was also proposed:

$$F \equiv \frac{\sum_i (\mathrm{Tr}\, H_i)^2}{n \sum_i \mathrm{Tr}\, H_i^2}. \tag{32}$$

In [12] F was used in a Finite Size Scaling analysis for the $(2, 0)$ geometry (see section 2.7 for developments in this area).
In order to interpret the observable F, it is useful to look at the $(2, 0)$ geometry explicitly. In this case F is:

$$F_{(2,0)} = \frac{(\mathrm{Tr}\, H_1)^2 + (\mathrm{Tr}\, H_2)^2}{n(\mathrm{Tr}\, H_1^2 + \mathrm{Tr}\, H_2^2)}. \tag{33}$$

In a plot of $\mathrm{Tr}\, H_1$ vs $\mathrm{Tr}\, H_2$ before, during and after the phase transition, it is clear that the observable F can be interpreted as the square of the radius of a circle (Fig.(5)). The behaviour for F was then analized systematically for higher geometries. The results are reported in Fig.(6).

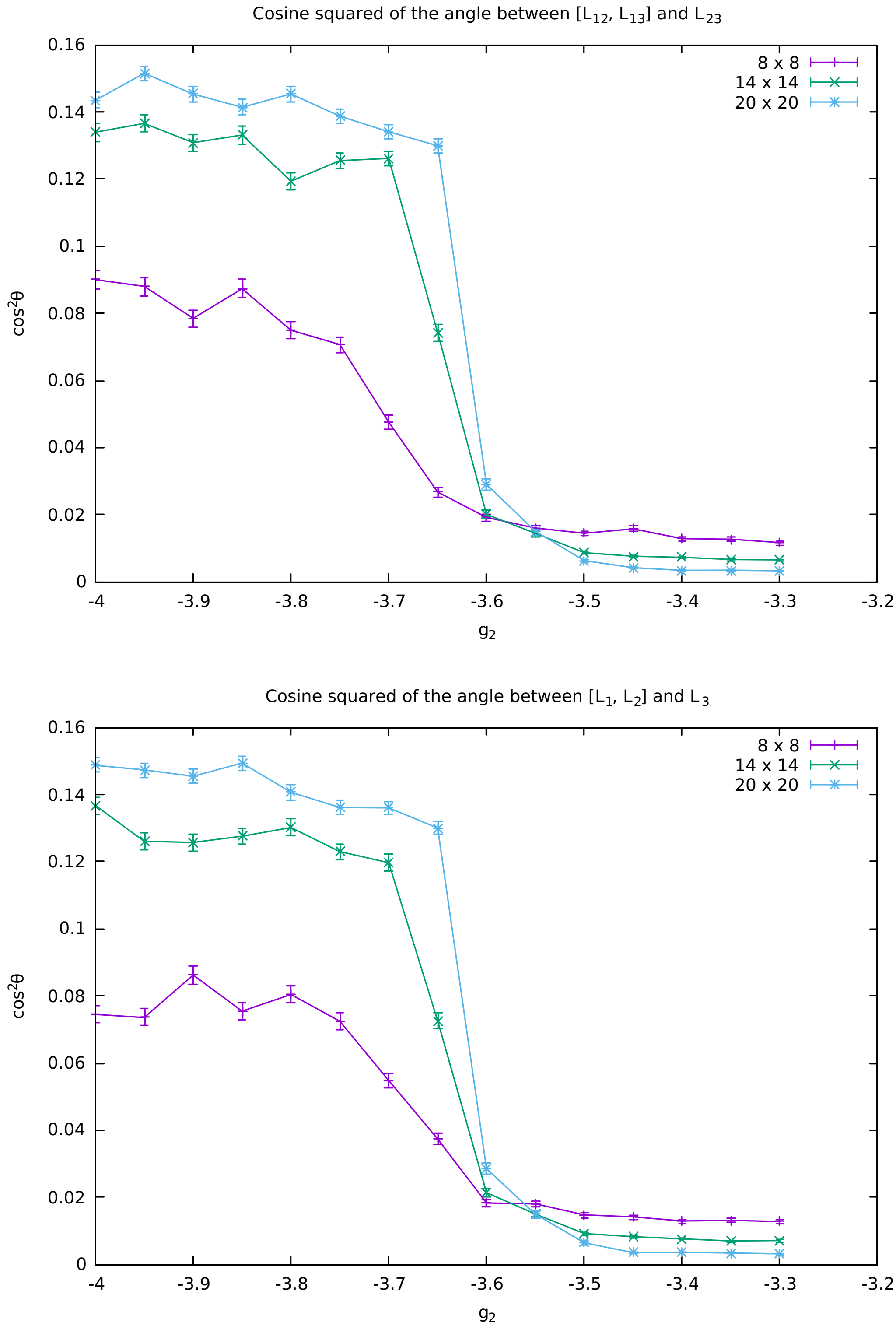

Figure 3: Cosine squared of the angle for the group of matrices L_{12}, L_{13}, L_{23} (top) and L_1, L_2, L_3 (bottom). The phase transition occurs between $g_2 = -3.7$ and $g_2 = -3.6$.

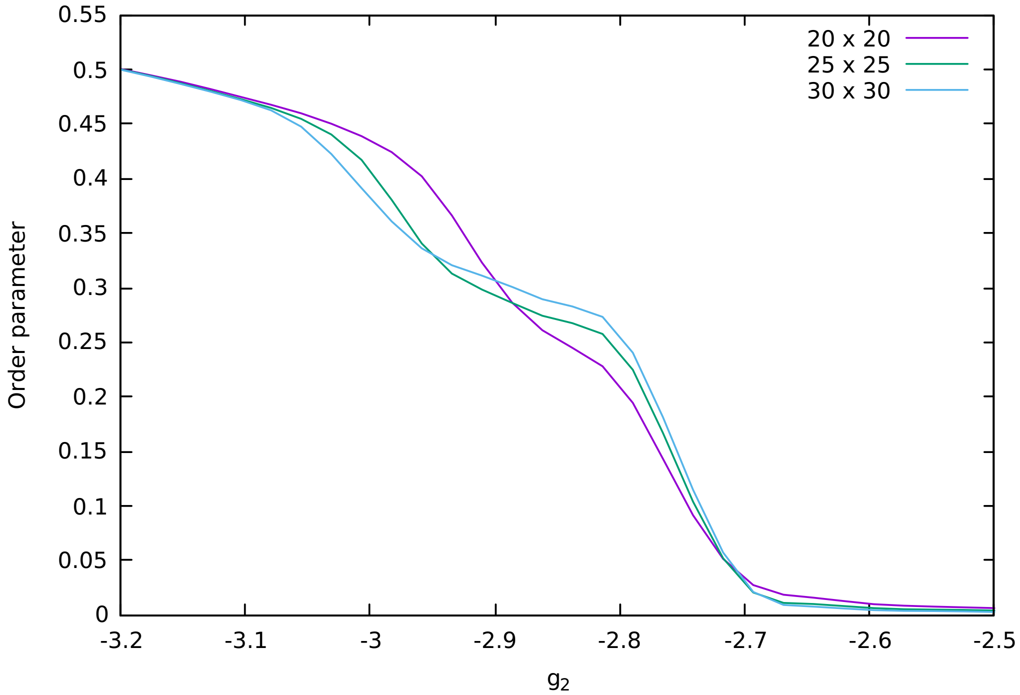

Figure 4: The $(2, 0)$ phase transition exhibits a double jump in the order parameter

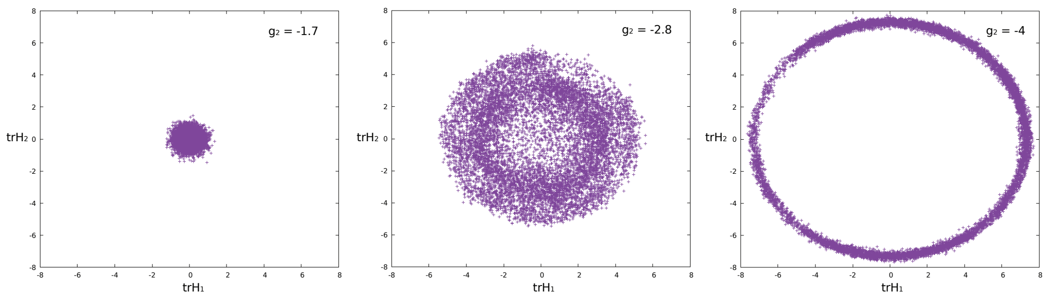

Figure 5: From left to right: $\mathrm{Tr}\, H_1$ vs $\mathrm{Tr}\, H_2$ before, during and after the $(2, 0)$ phase transition. Each point denotes a Monte Carlo step.

It seems to be the case that phase transitions in fuzzy spaces are driven by F developing a non-zero expectation value. However, in the next section it will be shown that in the case of the $(1,3)$ geometry an alternative observable built on the L matrices behaves like an order parameter for the phase transition. The implications of this dual description have not yet been object of study.

2.6 Algebraic structures forming in the $(1,3)$ phase transition

It has been argued in [3] that random fuzzy geometries might present a manifold-like behaviour close to phase transitions in the limit of infinite matrix size. A natural candidate for investigating this possibility is the $(1,3)$ random fuzzy space: it exhibits a phase transition [16] and it contains the fuzzy sphere as a particular case [2].

The most general Dirac operator of a $(1,3)$ fuzzy space is:

$$D_{13} = \gamma^0 \otimes \{H_0, \cdot\} + \gamma^1\gamma^2\gamma^3 \otimes \{H_{123}, \cdot\} + \sum_{i=1}^{3} \gamma^i \otimes [L_i, \cdot] + \sum_{j<k=1}^{3} \gamma^0\gamma^j\gamma^k \otimes [L_{jk}, \cdot] \tag{34}$$

where γ^0, γ^1, γ^2, γ^3 are the gamma matrices of an irreducible $(1,3)$ Clifford module (γ^0 is the Hermitian one).

The Dirac operator of a fuzzy sphere is:

$$D_{fs} = \gamma^0 \otimes I + \sum_{j<k=1}^{3} \gamma^0\gamma^j\gamma^k \otimes [L_{jk}, \cdot] \tag{35}$$

where L_{jk} are the standard generators of an irreducible n-dimensional representation of the Lie algebra $so(3)$.

A priori, when considering a random Dirac operator of the form D_{13}, the smallest algebra in which the L_{jk} matrices live is much bigger than $so(3)$. But if D_{13} is to resemble D_{fs} at the phase transition, then one would expect the algebra to shrink. In particular, the angle between $[L_{jk}, L_{lm}]$ and L_{pq} should decrease.

In order to test this hypotesis, every inequivalent angle[†] between $[L_\alpha, L_\beta]$ and L_γ has been measured close to the critical point, where L_α, L_β, L_γ are any of the L_i or L_{jk} matices of Eq.(34).

The results shown in Fig.(7) suggest that the three L_i matrices and the three L_{jk} matrices naturally split in two groups, and that in each group the angle

[†]The angle was defined using the Frobenius inner product: $\langle A, B\rangle = \operatorname{Tr} A^\dagger B$

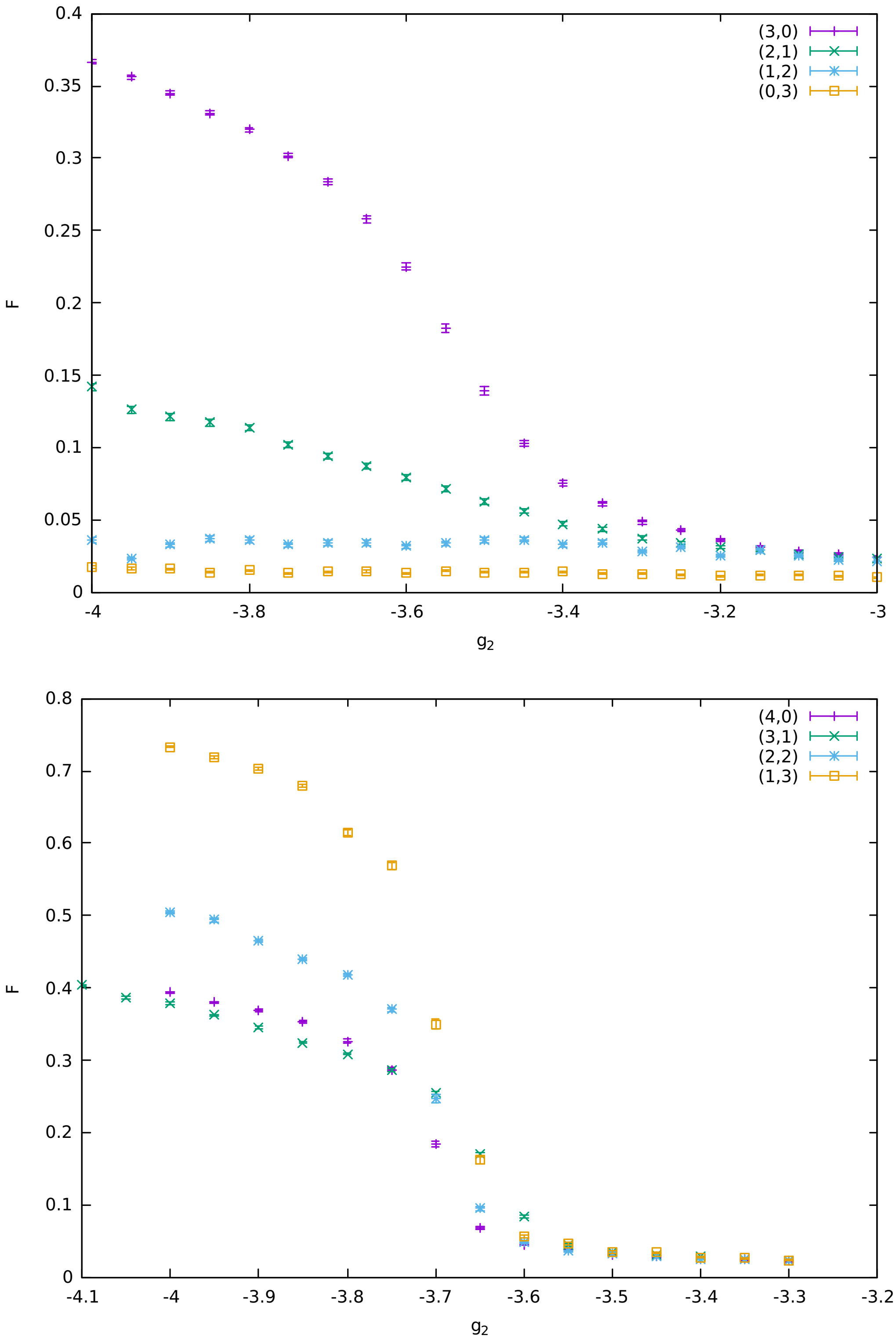

Figure 6: Observable F for $p+q = 3$ (top) and $p+q = 4$ geometries (bottom). Matrix size is 8×8.

at the phase transition decreases more and more as the matrix size increases.

2.7 The $(2,0)$ double jump phase transition

The $(2,0)$ fuzzy space is a useful toy model to explore the behaviour of random fuzzy spaces. In [12] the $(2,0)$ phase transition was studied by means of Finite Size Scaling. The results were compatible with the phase transition being in the universality class of the 3D Ising model or the 3D XY model.
The previous study was conducted with matrices up to size 15×15. In an attempt to better constrain the values of the critical exponents, new simulations have been perfomed with matrices of size 20×20, 25×25 and 30×30.
The new data (Fig.(8)) shows that the phase transition has in fact a richer structure, with a double jump. This feature is not observed in 3D Ising or XY model.

3 Future directions

As the field of random fuzzy spaces is reasonably new and unexplored, a lot can be done. The following plan for future lines of research includes both computational and theoretical aspects.
On the computational side, two (compatible) improvements of increasing complexity can be implemented:

1. Parallel Tempering: allows a more efficient and simultaneous exploration of the relevant Dirac operators in a range of coupling constants. Especially suited for the study of phase transitions.

2. Hamiltonian Monte Carlo: the standard algorithm for unquenched LQCD [18]. Faster than Metropolis, can be applied to any system with continuous parameter space.

On the theoretical side, two possible lines of research will be mentioned:

1. Finding a ground state for the $(1,3)$ geometry.

2. Characterize the $(2,0)$ phase transition.

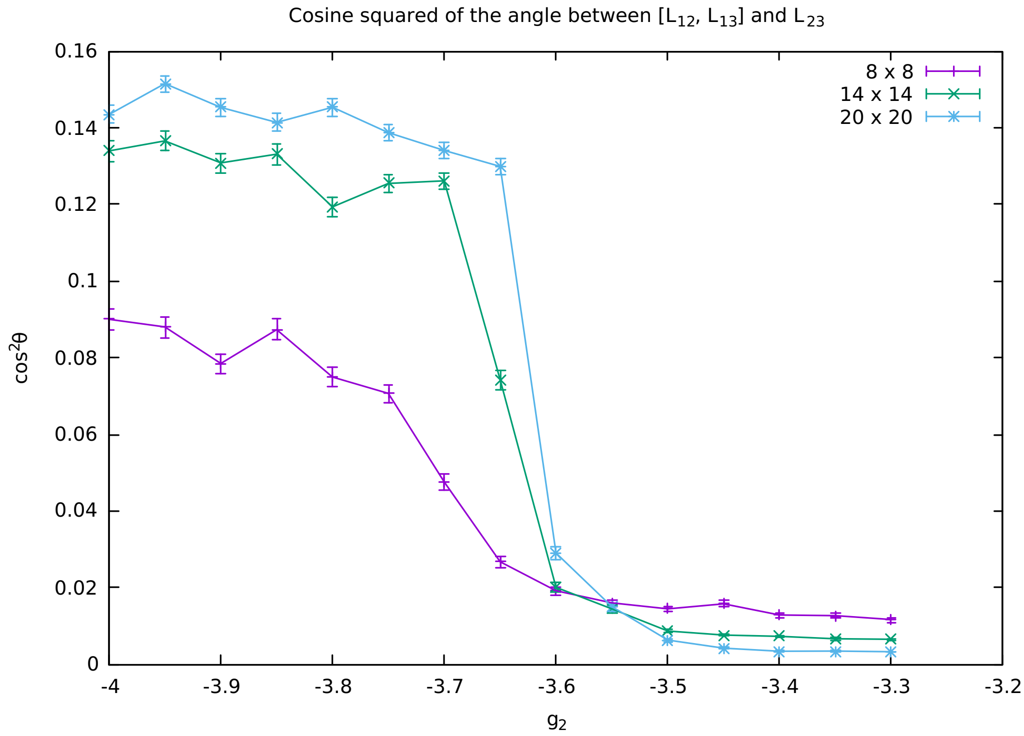

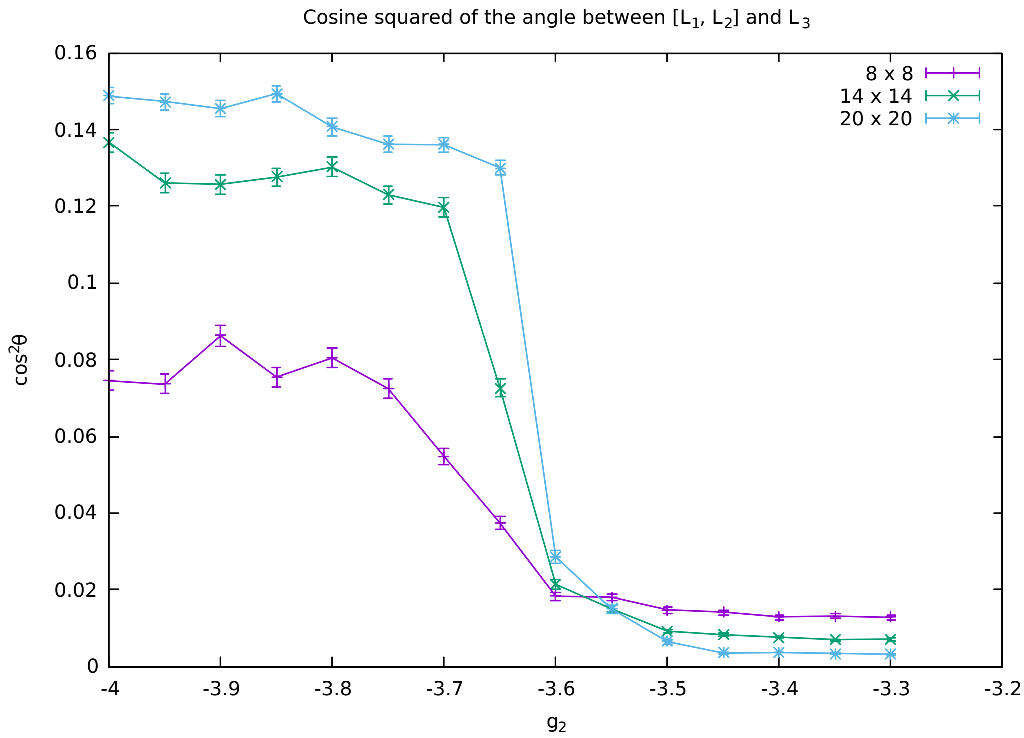

Figure 7: Cosine squared of the angle for the group of matrices L_{12}, L_{13}, L_{23} (top) and L_1, L_2, L_3 (bottom). The phase transition occurs between $g_2 = -3.7$ and $g_2 = -3.6$.

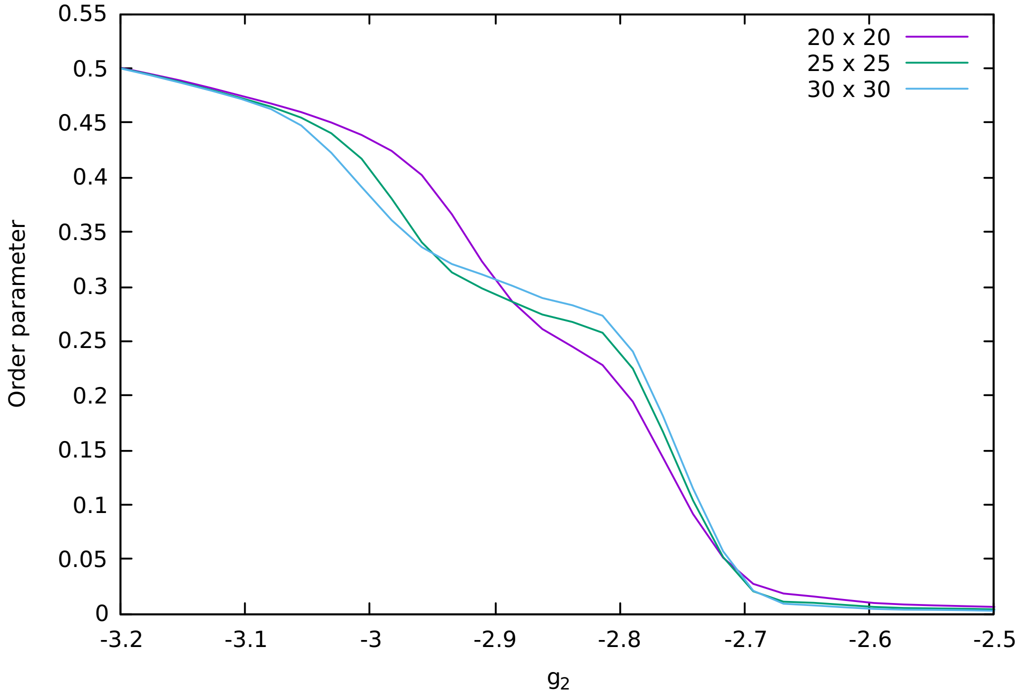

Figure 8: The $(2,0)$ phase transition exhibits a double jump in the order parameter

3.1 Parallel Tempering

A first version of parallel tempering was introduced in 1986 by Swendsen and Wang [21].
The idea behind it is to run parallel simulations of the system at different values of the coupling constant $g_1 < g_2 < \ldots < g_N$. After a certain number of iterations of the Monte Carlo algorithm, a configuration swap is proposed between adjacent systems g_i, g_{i+1} with probability:

$$p(i \leftrightarrow i+1) = \min\{1, \quad \exp[(g_{i+1} - g_i)(S[D_{i+1}] - S[D_i])]\}\,. \tag{36}$$

The swap preserves detailed balance [14], and therefore it does not affect the ergodicity of the Markov chain.
When studying phase transitions, one wants to run simulations in a range of coupling constants around the critical point. By tuning the separation between adjacent systems and swapping configurations as explained above, the autocorrelation time can drop significantly [6] yielding less correlated measurements.

3.2 Hamiltonian Monte Carlo

Hamiltonian Monte Carlo was introduced in 1987 to optimize Lattice QCD simulations with fermionic degrees of freedom [13]. The idea is to double up the space of parameters by introducing fictitious momenta and treating the Monte Carlo move proposal as Hamiltonian evolution in this new phase space.
The Hamiltonian function is built as follows. By denoting q_i the independent degrees of freedom of a Dirac operator D and p_i the fictitious conjugate momenta, the distribution (2) becomes:

$$e^{-S[D]} = e^{-S[q_i]} \quad \longrightarrow \quad e^{-(S[q_i]+K[p_i])} \equiv e^{-H[q_i,p_i]}. \tag{37}$$

The "kinetic energy" $K[p_i]$ is typically chosen to be of the form [19]:

$$K[p_i] = \sum_i \frac{p_i^2}{2m_i} \tag{38}$$

for positive m_i. A non-diagonal mass matrix can also be used [4].
The Hamiltonian Monte Carlo algorithm is comprised of three steps:

1. Draw the momenta p_i from their Gaussian distribution;

2. Evolve the system on phase space using Hamiltonian dynamics, obtaining new parameters q_i', p_i';

3. Accept the new state with probability:

$$\min\left\{1, \quad \exp\left(H[q_i, p_i] - H[q_i', p_i']\right)\right\}.$$

If the move is accepted, the parameters q_i' will then define a new Dirac operator D' that is much less correlated to D compared to a typical Metropolis move.
Notes:

1. Resampling the momenta at each iteration ensures that the exploration is not confined to a single "energy" orbit in phase space.

2. The numerical integration of Hamilton equations is usually done using symplectic integrators, the most common choice being the leapfrog method [4]. Free parameters of the integrator are the stepsize ϵ and the total number L of integration steps.

3. Compared to Metropolis, Hamiltonian Monte Carlo has a higher number of free parameters that need tuning for optimal performance: m_i, ϵ and L.

3.3 A ground state for the $(1, 3)$ geometry

The results of section 2.6 seem to suggest that on one side of the phase transition the L matrices of a typical $(1, 3)$ Dirac operator form some sort of non-trivial algebraic structure.
A possibility is that, in the limit of infinite matrix size, the typical Dirac operator looks like the fuzzy sphere of Eq.(35). However, the degeneracy in the spectrum of the fuzzy sphere makes an exact correspondence unlikely†.
Further simulations could help in making a plausible guess for the ground state, around which the path integral can be expanded in Feynman diagrams.
Another way of finding the ground state goes through the minimization of an effective action, since a simple minimization of the bare action would not take into account the volume of the gauge orbits. A useful analogy is the problem of finding the typical radius in:

$$\int e^{-(x^2+y^2)} dx dy.$$

Minimizing $x^2 + y^2$ gives $r = 0$, whereas in polar coordinates the volume of the orbits is explicitly given by the Jacobian, which can be included in the

†This is because of the phenomenon of eigenvalue repulsion in random matrix models

exponential:

$$\int e^{-r^2+\log r} dr d\theta.$$

The minimum of the "effective potential" $r^2 - \log r$ is now different from zero, and represents the typical value of the radius.
In the case of Dirac operators, one expects to write an effective action by introducing anticommuting ghost fields.

3.4 Characterization of the $(2,0)$ phase transition

Although the $(2,0)$ geometry is of limited interest from a quantum gravity viewpoint, the newly discovered "double jump" can be an interesting feature in itself.
Most notably, the same phenomenon has been predicted in 1960 by Erdős and Rényi for a certain model of random graphs [15]. Since then, this behaviour has been observed in other models of clustered networks, for example [5] and [9]. A potential link between random fuzzy spaces and random graphs might be an interesting topic to explore.
On the other hand, double jumps are not limited to random graphs. In [22] such behaviour is observed in a modified XY model with a purely nematic Hamiltonian.

As the field of random fuzzy spaces is reasonably new and unexplored, a lot can be done. The following plan for future lines of research includes both computational and theoretical aspects.
On the computational side, two (compatible) improvements of increasing complexity can be implemented:

1. Parallel Tempering: allows a more efficient and simultaneous exploration of the relevant Dirac operators in a range of coupling constants. Especially suited for the study of phase transitions.

2. Hamiltonian Monte Carlo: the standard algorithm for unquenched LQCD [18]. Faster than Metropolis, can be applied to any system with continuous parameter space.

On the theoretical side, two possible lines of research will be mentioned:

1. Finding a ground state for the $(1,3)$ geometry.

2. Characterize the $(2,0)$ phase transition.

3.5 Parallel Tempering

A first version of parallel tempering was introduced in 1986 by Swendsen and Wang [21].
The idea behind it is to run parallel simulations of the system at different values of the coupling constant $g_1 < g_2 < \ldots < g_N$. After a certain number of iterations of the Monte Carlo algorithm, a configuration swap is proposed between adjacent systems g_i, g_{i+1} with probability:

$$p(i \leftrightarrow i+1) = \min\left\{1, \quad \exp\left[(g_{i+1} - g_i)(S[D_{i+1}] - S[D_i])\right]\right\}. \tag{39}$$

The swap preserves detailed balance [14], and therefore it does not affect the ergodicity of the Markov chain.
When studying phase transitions, one wants to run simulations in a range of coupling constants around the critical point. By tuning the separation between adjacent systems and swapping configurations as explained above, the autocorrelation time can drop significantly [6] yielding less correlated measurements.

3.6 Hamiltonian Monte Carlo

Hamiltonian Monte Carlo was introduced in 1987 to optimize Lattice QCD simulations with fermionic degrees of freedom [13]. The idea is to double up the space of parameters by introducing fictitious momenta and treating the Monte Carlo move proposal as Hamiltonian evolution in this new phase space.
The Hamiltonian function is built as follows. By denoting q_i the independent degrees of freedom of a Dirac operator D and p_i the fictitious conjugate momenta, the distribution (2) becomes:

$$e^{-S[D]} = e^{-S[q_i]} \quad \longrightarrow \quad e^{-(S[q_i]+K[p_i])} \equiv e^{-H[q_i,p_i]}. \tag{40}$$

The "kinetic energy" $K[p_i]$ is typically chosen to be of the form [19]:

$$K[p_i] = \sum_i \frac{p_i^2}{2m_i} \tag{41}$$

for positive m_i. A non-diagonal mass matrix can also be used [4].
The Hamiltonian Monte Carlo algorithm is comprised of three steps:

1. Draw the momenta p_i from their Gaussian distribution;
2. Evolve the system on phase space using Hamiltonian dynamics, obtaining new parameters q_i', p_i';

3. Accept the new state with probability:

$$\min \{1, \quad \exp \left(H[q_i, p_i] - H[q_i', p_i']\right)\}.$$

If the move is accepted, the parameters q_i' will then define a new Dirac operator D' that is much less correlated to D compared to a typical Metropolis move.
Notes:

1. Resampling the momenta at each iteration ensures that the exploration is not confined to a single "energy" orbit in phase space.

2. The numerical integration of Hamilton equations is usually done using symplectic integrators, the most common choice being the leapfrog method [4]. Free parameters of the integrator are the stepsize ϵ and the total number L of integration steps.

3. Compared to Metropolis, Hamiltonian Monte Carlo has a higher number of free parameters that need tuning for optimal performance: m_i, ϵ and L.

3.7 A ground state for the $(1, 3)$ geometry

The results of section 2.6 seem to suggest that on one side of the phase transition the L matrices of a typical $(1, 3)$ Dirac operator form some sort of non-trivial algebraic structure.
A possibility is that, in the limit of infinite matrix size, the typical Dirac operator looks like the fuzzy sphere of Eq.(35). However, the degeneracy in the spectrum of the fuzzy sphere makes an exact correspondence unlikely†. Further simulations could help in making a plausible guess for the ground state, around which the path integral can be expanded in Feynman diagrams. Another way of finding the ground state goes through the minimization of an effective action, since a simple minimization of the bare action would not take into account the volume of the gauge orbits. A useful analogy is the problem of finding the typical radius in:

$$\int e^{-(x^2+y^2)} dx dy.$$

Minimizing $x^2 + y^2$ gives $r = 0$, whereas in polar coordinates the volume of the orbits is explicitly given by the Jacobian, which can be included in the

†This is because of the phenomenon of eigenvalue repulsion in random matrix models

exponential:

$$\int e^{-r^2+\log r} dr d\theta.$$

The minimum of the "effective potential" $r^2 - \log r$ is now different from zero, and represents the typical value of the radius.
In the case of Dirac operators, one expects to write an effective action by introducing anticommuting ghost fields.

3.8 Characterization of the $(2, 0)$ phase transition

Although the $(2, 0)$ geometry is of limited interest from a quantum gravity viewpoint, the newly discovered "double jump" can be an interesting feature in itself.
Most notably, the same phenomenon has been predicted in 1960 by Erdős and Rényi for a certain model of random graphs [15]. Since then, this behaviour has been observed in other models of clustered networks, for example [5] and [9]. A potential link between random fuzzy spaces and random graphs might be an interesting topic to explore.
On the other hand, double jumps are not limited to random graphs. In [22] such behaviour is observed in a modified XY model with a purely nematic Hamiltonian.

As the field of random fuzzy spaces is reasonably new and unexplored, a lot can be done. The following plan for future lines of research includes both computational and theoretical aspects.
On the computational side, two (compatible) improvements of increasing complexity can be implemented:

1. Parallel Tempering: allows a more efficient and simultaneous exploration of the relevant Dirac operators in a range of coupling constants. Especially suited for the study of phase transitions.

2. Hamiltonian Monte Carlo: the standard algorithm for unquenched LQCD [18]. Faster than Metropolis, can be applied to any system with continuous parameter space.

On the theoretical side, two possible lines of research will be mentioned:

1. Finding a ground state for the $(1, 3)$ geometry.

2. Characterize the $(2, 0)$ phase transition.

3.9 Parallel Tempering

A first version of parallel tempering was introduced in 1986 by Swendsen and Wang [21].
The idea behind it is to run parallel simulations of the system at different values of the coupling constant $g_1 < g_2 < \ldots < g_N$. After a certain number of iterations of the Monte Carlo algorithm, a configuration swap is proposed between adjacent systems g_i, g_{i+1} with probability:

$$p(i \leftrightarrow i+1) = \min \{1, \quad \exp\left[(g_{i+1} - g_i)(S[D_{i+1}] - S[D_i])\right]\} . \tag{42}$$

The swap preserves detailed balance [14], and therefore it does not affect the ergodicity of the Markov chain.
When studying phase transitions, one wants to run simulations in a range of coupling constants around the critical point. By tuning the separation between adjacent systems and swapping configurations as explained above, the autocorrelation time can drop significantly [6] yielding less correlated measurements.

3.10 Hamiltonian Monte Carlo

Hamiltonian Monte Carlo was introduced in 1987 to optimize Lattice QCD simulations with fermionic degrees of freedom [13]. The idea is to double up the space of parameters by introducing fictitious momenta and treating the Monte Carlo move proposal as Hamiltonian evolution in this new phase space.
The Hamiltonian function is built as follows. By denoting q_i the independent degrees of freedom of a Dirac operator D and p_i the fictitious conjugate momenta, the distribution (2) becomes:

$$e^{-S[D]} = e^{-S[q_i]} \quad \longrightarrow \quad e^{-(S[q_i]+K[p_i])} \equiv e^{-H[q_i,p_i]}. \tag{43}$$

The "kinetic energy" $K[p_i]$ is typically chosen to be of the form [19]:

$$K[p_i] = \sum_i \frac{p_i^2}{2m_i} \tag{44}$$

for positive m_i. A non-diagonal mass matrix can also be used [4].
The Hamiltonian Monte Carlo algorithm is comprised of three steps:

1. Draw the momenta p_i from their Gaussian distribution;
2. Evolve the system on phase space using Hamiltonian dynamics, obtaining new parameters q_i', p_i';

3. Accept the new state with probability:

$$\min\{1, \quad \exp(H[q_i, p_i] - H[q_i', p_i'])\}\,.$$

If the move is accepted, the parameters q_i' will then define a new Dirac operator D' that is much less correlated to D compared to a typical Metropolis move.
Notes:

1. Resampling the momenta at each iteration ensures that the exploration is not confined to a single "energy" orbit in phase space.

2. The numerical integration of Hamilton equations is usually done using symplectic integrators, the most common choice being the leapfrog method [4]. Free parameters of the integrator are the stepsize ϵ and the total number L of integration steps.

3. Compared to Metropolis, Hamiltonian Monte Carlo has a higher number of free parameters that need tuning for optimal performance: m_i, ϵ and L.

3.11 A ground state for the $(1, 3)$ geometry

The results of section 2.6 seem to suggest that on one side of the phase transition the L matrices of a typical $(1, 3)$ Dirac operator form some sort of non-trivial algebraic structure.
A possibility is that, in the limit of infinite matrix size, the typical Dirac operator looks like the fuzzy sphere of Eq.(35). However, the degeneracy in the spectrum of the fuzzy sphere makes an exact correspondence unlikely†. Further simulations could help in making a plausible guess for the ground state, around which the path integral can be expanded in Feynman diagrams. Another way of finding the ground state goes through the minimization of an effective action, since a simple minimization of the bare action would not take into account the volume of the gauge orbits. A useful analogy is the problem of finding the typical radius in:

$$\int e^{-(x^2+y^2)} dx dy.$$

Minimizing $x^2 + y^2$ gives $r = 0$, whereas in polar coordinates the volume of the orbits is explicitly given by the Jacobian, which can be included in the

†This is because of the phenomenon of eigenvalue repulsion in random matrix models

exponential:

$$\int e^{-r^2+\log r} dr d\theta.$$

The minimum of the "effective potential" $r^2 - \log r$ is now different from zero, and represents the typical value of the radius.
In the case of Dirac operators, one expects to write an effective action by introducing anticommuting ghost fields.

3.12 Characterization of the $(2,0)$ phase transition

Although the $(2,0)$ geometry is of limited interest from a quantum gravity viewpoint, the newly discovered "double jump" can be an interesting feature in itself.
Most notably, the same phenomenon has been predicted in 1960 by Erdős and Rényi for a certain model of random graphs [15]. Since then, this behaviour has been observed in other models of clustered networks, for example [5] and [9]. A potential link between random fuzzy spaces and random graphs might be an interesting topic to explore.
On the other hand, double jumps are not limited to random graphs. In [22] such behaviour is observed in a modified XY model with a purely nematic Hamiltonian.

Appendix A: Notation

1. To avoid dealing with both Hermitian and anti-Hermitian matrices in Eq.(1), it is convenient to redefine $i\tilde{L}_j \equiv L_j$ and $\tilde{\alpha}_j \equiv i\alpha_j$. Eq.(1) becomes:
$$D = \sum_j \tilde{\alpha}_j \otimes [\tilde{L}_j, \cdot] + \sum_k \tau_k \otimes \{H_k, \cdot\} \tag{45}$$
and all the matrices are Hermitian.

2. Commutators and anti-commutators are represented in matrix form as:
$$[A, \cdot] = A \otimes I - I \otimes A^T$$
$$\{A, \cdot\} = A \otimes I + I \otimes A^T.$$
As a shorthand, the following notation will be used:
$$[A, \cdot]_\epsilon \equiv A \otimes I + \epsilon\, I \otimes A^T.$$

The final form of Eq.(1) is then:

$$D = \sum_{i \in I} \omega_i \otimes [M_i, \cdot]_{\epsilon_i} \tag{46}$$

for Hermitian matrices M_i, with $\omega_i \in \{\tilde{\alpha}_j\} \cup \{\tau_k\}$, and $\epsilon_i = \pm 1$ depending on ω_i being a τ matrix or a $\tilde{\alpha}$ matrix.

Appendix B: Matrix derivatives

Let $A \in M_n(\mathbb{C})$ and $f(A)$ be a complex valued function of A. The derivative of f with respect to A is defined in components as the $n \times n$ matrix:

$$\left(\frac{\partial f}{\partial A}\right)_{lm} \equiv \frac{\partial f}{\partial A_{lm}}. \tag{47}$$

The two special cases of interest here are:

$$\frac{\partial \operatorname{Tr} A}{\partial A} = I \tag{48}$$

$$\frac{\partial \operatorname{Tr} AB}{\partial A} = B^T. \tag{49}$$

Appendix C

The explicit form of $\mathcal{B}_k(i,i,k)$, $\mathcal{B}_k(i,k,i)$ and $\mathcal{B}_k(k,k,k)$ is given.

$$\begin{aligned} \mathcal{B}_k(i,i,k) &= \operatorname{Tr}(\omega_k\omega_i\omega_i\omega_k)A(k,i,i,k)^T = CA(k,i,i,k)^T \\ \mathcal{B}_k(i,k,i) &= \operatorname{Tr}(\omega_k\omega_i\omega_k\omega_i)A(k,i,k,i)^T \\ \mathcal{B}_k(k,k,k) &= \operatorname{Tr}(\omega_k\omega_k\omega_k\omega_k)A(k,k,k,k)^T = CA(k,k,k,k)^T \end{aligned} \tag{50}$$

where C is the dimension of the Clifford module and the A matrices are:

$$\begin{aligned} A(k,i,i,k) = n&[1+\dagger]M_i^2 M_k + \\ &2\epsilon_k I \operatorname{Tr} M_i^2 M_k + \\ &2\epsilon_i \operatorname{Tr} M_i[1+\dagger]M_i M_k + \\ &4\epsilon_k\epsilon_i M_i \operatorname{Tr} M_i M_k + \\ &2\epsilon_k M_i^2 \operatorname{Tr} M_k + \\ &2M_k \operatorname{Tr} M_i^2 \end{aligned} \tag{51}$$

$$
\begin{aligned}
A(k,i,k,i) = {} & 2nM_iM_kM_i + \\
& 2\epsilon_k I \operatorname{Tr} M_i^2 M_k + \\
& 2\epsilon_i \operatorname{Tr} M_i [1+\dagger] M_i M_k + \\
& 4\epsilon_k \epsilon_i M_i \operatorname{Tr} M_i M_k + \\
& 2\epsilon_k M_i^2 \operatorname{Tr} M_k + \\
& 2M_k \operatorname{Tr} M_i^2
\end{aligned} \tag{52}
$$

$$
\begin{aligned}
A(k,k,k,k) = {} & 2nM_k^3 + 2\epsilon_k I \operatorname{Tr} M_k^3 + \\
& 6M_k \operatorname{Tr} M_k^2 + 6\epsilon_k M_k^2 \operatorname{Tr} M_k.
\end{aligned} \tag{53}
$$

Appendix C

Using the following notation:

$$
D = \sum_{i\in I} \omega_i \otimes [M_i, \cdot]_{\epsilon_i} \tag{54}
$$

$$
\delta D = \omega_x \otimes [m_x, \cdot]_{\epsilon_x} \tag{55}
$$

$$
[M, \cdot]_\epsilon = \sum_{q=0}^{1} \epsilon^{1-q} M^q \otimes (M^T)^{1-q} \tag{56}
$$

where $x \in I$ is a fixed index and m_x is a random Hermitian matrix, Eq.(**??**) becomes:

$$
\begin{aligned}
(D')^p - D^p = & \sum_{s=1}^{p} \sum_{i_1,..,i_{p-s}\in I} \sum_{\substack{k_1,..,k_{p-s}=0 \\ \sum k_j \le s}}^{s} \sum_{\substack{l_1,..,l_{p-s}=0 \\ l_j \le k_j}}^{s} \sum_{l'=0}^{s-\sum k_j} \sum_{q_1,..,q_{p-s}=0}^{1} \cdot \Bigg[\\
& \cdot \Bigg[\binom{k_1}{l_1} \dots \binom{k_{p-s}}{l_{p-s}} \binom{s-\sum k_j}{l'} (\epsilon_x)^{s-\sum l_j - l'} (\epsilon_{i_1})^{1-q_1} \dots (\epsilon_{i_{p-s}})^{1-q_{p-s}} \cdot \\
& \cdot \quad (\omega_x)^{k_1} \omega_{i_1} \dots (\omega_x)^{k_{p-s}} \omega_{i_{p-s}} (\omega_x)^{s-\sum k_j} \quad \otimes \\
& (m_x)^{l_1} (M_{i_1})^{q_1} \dots (m_x)^{l_{p-s}} (M_{i_{p-s}})^{q_{p-s}} (m_x)^{l'} \quad \otimes \\
& (m_x^T)^{k_1-l_1} (M_{i_1}^T)^{1-q_1} \dots (m_x^T)^{k_{p-s}-l_{p-s}} (M_{i_{p-s}}^T)^{1-q_{p-s}} (m_x^T)^{s-\sum k_j - l'} \Bigg].
\end{aligned} \tag{57}
$$

Appendix D

Suppose m_x has the following form:

$$(m_x)_{ij} = z\delta_{iI}\delta_{jJ} + z^*\delta_{iJ}\delta_{jI} \tag{58}$$

where z is a complex number, δ_{ij} is the Kronecker delta, and I, J are the indices of the only non-vanishing entries: $(m_x)_{IJ} = (m_x)^*_{JI} = z \neq 0$.
If n is the dimension of the matrix algebra and C is the dimension of the Clifford module, then for $p = 2$:

1. if $I \neq J$:

$$\mathrm{Tr}[(D')^2 - D^2] = 4\ C\ n\ [\ 2\,\mathrm{Re}(z(M_x)_{JI}) + |z|^2\ ] \tag{59}$$

2. if $I = J$:

$$\mathrm{Tr}[(D')^2 - D^2] = 8\,C\ \mathrm{Re}(z)\,[\,n\,(\,\mathrm{Re}(M_x)_{II} + \mathrm{Re}(z)\,) + \epsilon_x(\mathrm{Tr}\,M_x + \mathrm{Re}(z))] \tag{60}$$

While for $p = 4$:

1. if $I \neq J$:

$$\operatorname{Tr} D^3 \delta D = \sum_{\substack{i_1 < i_3 \\ i_2}} 2 \operatorname{Re} \operatorname{Tr}(A[i_1, i_2, i_3, x]) + \sum_i \operatorname{Re} \operatorname{Tr}(A[i, x, i, x])$$

$$\begin{aligned}
A[i_1, i_2, i_3, x] = \operatorname{Tr}(\omega_{i_1}\omega_{i_2}\omega_{i_3}\omega_x)\Big[& \\
& n[1 + \epsilon_{i_1}\epsilon_{i_2}\epsilon_{i_3}\epsilon_x *][(M_{i_1}M_{i_2}M_{i_3})_{JI} z + (M_{i_1}M_{i_2}M_{i_3})_{IJ} z^*] + \\
\sum_{\{\alpha,\beta,\gamma\}} & [\epsilon_\gamma + \epsilon_\alpha\epsilon_\beta\epsilon_x *][(M_\alpha M_\beta)_{JI} z + (M_\alpha M_\beta)_{IJ} z^*] + \\
& [\epsilon_\alpha\epsilon_\beta + \epsilon_\gamma\epsilon_x] 2 \operatorname{Re}((M_\gamma)_{JI} z) \operatorname{Tr} M_\alpha M_\beta)\Big] \qquad (61) \\
\text{with} \quad & \{\alpha, \beta, \gamma\} = \{i_1, i_2, i_3\}, \{i_1, i_3, i_2\}, \{i_2, i_3, i_1\}
\end{aligned}$$

$$\begin{aligned}
\operatorname{Tr} D^2 (\delta D)^2 = \sum_i C \Big[& |z|^2 [2n((M_i^2)_{II} + (M_i^2)_{JJ}) + \\
& 4\epsilon_i \operatorname{Tr} M_i((M_i)_{II} + (M_i)_{JJ}) + \\
& 4 \operatorname{Tr} M_i^2] + 16\epsilon_i\epsilon_x \operatorname{Re}((M_i)_{JI} z)^2 \Big] \qquad (62)
\end{aligned}$$

$$\begin{aligned}
\operatorname{Tr} D\delta D D \delta D = \sum_i \operatorname{Tr}(\omega_i\omega_x\omega_i\omega_x) \Big[& 4n(\operatorname{Re}((M_i)_{JI}^2 z^2) + \\
& |z|^2 \operatorname{Re}((M_i)_{II}(M_i)_{JJ}) + \\
& |z|^2 [4\epsilon_i \operatorname{Tr} M_i((M_i)_{II} + (M_i)_{JJ}) + 4 \operatorname{Tr} M_i^2] + \\
& 16\epsilon_i\epsilon_x \operatorname{Re}((M_i)_{JI} z)^2 \Big] \qquad (63)
\end{aligned}$$

$$\operatorname{Tr} D(\delta D)^3 = 4C(n+6)|z|^2 \operatorname{Re}((M_x)_{JI} z) \qquad (64)$$

$$\operatorname{Tr}(\delta D)^4 = 4C(n+6)|z|^4 \qquad (65)$$

2. if $I = J$:

$$\operatorname{Tr} D^3 \delta D = \sum_{\substack{i_1 < i_3 \\ i_2}} 2 \operatorname{Re} \operatorname{Tr}(A[i_1, i_2, i_3, x]) + \sum_i \operatorname{Re} \operatorname{Tr}(A[i, x, i, x])$$

$$\begin{aligned} A[i_1, i_2, i_3, x] = \operatorname{Tr}(\omega_{i_1}\omega_{i_2}\omega_{i_3}\omega_x) 2 \operatorname{Re} z \Big[& \\ n[1 + \epsilon_{i_1}\epsilon_{i_2}\epsilon_{i_3}\epsilon_x *](M_{i_1} M_{i_2} M_{i_3})_{II} + & \\ [\epsilon_x + \epsilon_{i_1}\epsilon_{i_2}\epsilon_{i_3} *] \operatorname{Tr} M_{i_1} M_{i_2} M_{i_3} + & \\ \sum_{\{\alpha,\beta,\gamma\}} [\epsilon_\gamma + \epsilon_\alpha \epsilon_\beta \epsilon_x *](M_\alpha M_\beta)_{II} \operatorname{Tr} M_\gamma + & \\ [\epsilon_\alpha \epsilon_\beta + \epsilon_\gamma \epsilon_x](M_\gamma)_{II} \operatorname{Tr} M_\alpha M_\beta) \Big] & \qquad (66) \\ \text{with} \quad \{\alpha, \beta, \gamma\} = \{i_1, i_2, i_3\}, \{i_1, i_3, i_2\}, \{i_2, i_3, i_1\} & \end{aligned}$$

$$\begin{aligned} \operatorname{Tr} D^2 (\delta D)^2 = \sum_i C (\operatorname{Re} z)^2 \Big[& 2n(M_i)_{II} + 4\epsilon_x (M_i^2)_{II} + \\ & 4\epsilon_i (M_i)_{II} \operatorname{Tr} M_i + 4\epsilon_i \epsilon_x (M_i)_{II}^2 + 2 \operatorname{Tr} M_i^2 \Big] \end{aligned} \qquad (67)$$

$$\begin{aligned} \operatorname{Tr} D \delta D D \delta D = \sum_i \operatorname{Tr}(\omega_i \omega_x \omega_i \omega_x)(\operatorname{Re} z)^2 \Big[& 2n(M_i)_{II} + 4\epsilon_x (M_i^2)_{II} + \\ & 4\epsilon_i (M_i)_{II} \operatorname{Tr} M_i + 4\epsilon_i \epsilon_x (M_i)_{II}^2 + 2 \operatorname{Tr} M_i^2 \Big] \end{aligned} \qquad (68)$$

$$\operatorname{Tr} D (\delta D)^3 = 16 C (\operatorname{Re} z)^3 ((n + 3\epsilon_x + 3)(M_x)_{II} + \epsilon_x \operatorname{Tr} M_x) \qquad (69)$$

$$\operatorname{Tr}(\delta D)^4 = 32 C (n + 4\epsilon_x + 3)(\operatorname{Re} z)^4 \qquad (70)$$

References

[1] J. W. Barrett, "Lorentzian version of the noncommutative geometry of the standard model of particle physics", *J. Math. Phys.* **48**, 012303 (2007).

[2] J. W. Barrett, "Matrix geometries and fuzzy spaces as finite spectral triples", *J. Math. Phys.* **56**, 082301 (2015).

[3] J. W. Barrett and L. Glaser, "Monte Carlo simulations of random non-commutative geometries", *J. Phys. A* **49**, 24, 245001 (2016).

[4] M. Betancourt, "A Conceptual Introduction to Hamiltonian Monte Carlo", (arXiv:1701.02434v1, 2017).

[5] U. Bhat, M. Shrestha and L. Hébert-Dufresne, "Exotic phase transitions of k-cores in clustered networks", *Phys. Rev. E* **95**, 012314 (2017).

[6] E. Bittner and W. Janke, "Parallel-tempering cluster algorithm for computer simulations of critical phenomena", *Phys. Rev. E* **84**, 036701 (2011).

[7] A. H. Chamseddine and A. Connes, "The spectral action principle", *Commun. Math. Phys.* **186**, 731–750 (1997).

[8] A. H. Chamseddine, A. Connes and M. Marcolli, "Gravity and the standard model with neutrino mixing", *Adv. Theor. Math. Phys.* **11**, 991–1089 (2007).

[9] P. Colomer-de-Simón and M. Boguñá, "Double Percolation Phase Transition in Clustered Complex Networks", *Phys. Rev. X* **4**, 041020 (2014).

[10] A. Connes, "Gravity coupled with matter and the foundation of noncommutative geometry", *Commun. Math. Phys.* **183**, 1, 155–176 (1996).

[11] A. Connes, "On the spectral characterization of manifolds", *J. Noncommut. Geom.* **7**, 1–82 (2013).

[12] M. D'Arcangelo, *Random Non-Commutative Geometries* (Unpublished master's thesis, 2017).

[13] S. Duane, A. D. Kennedy, B. J. Pendleton and D. Roweth, "Hybrid Monte Carlo", *Phys. Lett. B* **195**, 216–222 (1987).

[14] D. J. Earl and M. W. Deem, "Parallel tempering: Theory, applications, and new perspectives", *Phys. Chem. Chem. Phys.* **7**, 3910–3916 (2005).

[15] P. Erdős and A. Rényi, "On the Evolution of Random Graphs", *Publication of the Mathematical Institute of the Hungarian Academy of Sciences* 17–61 (1960).

[16] L. Glaser, "Scaling behaviour in random non-commutative geometries", *J. Phys. A* **50**, 27, 275201 (2017).

[17] W. K. Hastings, "Monte Carlo sampling methods using Markov chains and their applications", *Biometrika* **57**, 1, 97–109 (1970).

[18] I. Montvay and G. Munster, *Quantum Fields on a Lattice* (Cambridge University Press, 2009).

[19] R. M. Neal, *Handbook of Markov Chain Monte Carlo* (Chapman & Hall / CRC Press, 2011).

[20] W. D. Suijlekom, *Noncommutative Geometry and Particle Physics* (Springer, 2014).

[21] R. H. Swendsen and J. -S. Wang, "Replica Monte Carlo Simulation of Spin-Glasses", *Phys. Rev. Lett.* **57**, 1, 2607 (1986).

[22] M. Žukovič and G. Kalagov, "Magnetic quasi-long-range ordering in nematic systems due to competition between higher-order couplings", *Phys. Rev. E* **97**, 052101 (2018).